ACS Catalysis

Editors' Choice
Open Access

pubs.acs.org/acscatalysis
Research Article

Commercial Group III–V Metal Alkoxide Catalysts for Selective Epoxide and Anhydride Ring Opening Copolymerization Delivering Poly(ester-*alt*-ethers)

Ryan W. F. Kerr, Alexander R. Craze, and Charlotte K. Williams*

Cite This: *ACS Catal.* 2026, 16, 5673–5681
Read Online

ACCESS | Metrics & More | Article Recommendations | Supporting Information

ABSTRACT: The ring-opening copolymerization (ROCOP) of cyclic anhydrides (*A*) and epoxides (*B*) is a controlled route to alternating polyesters, with the best catalysts delivering high ester sequence (*AB*) selectivity. In contrast, very few catalysts can selectively enchain the same monomers to produce ester-*alt*-ether (*ABB*) sequences. Here, simple, commercial, homoleptic Zr(IV) catalysts (alkoxides and chloride) show faster rates, controlled polymerization and high selectivity in epoxide/anhydride ROCOP to selectively produce poly(ester-*alt*-ethers) (>95%); they outperform the best prior Zr(IV) coordination catalyst. Comparing the copolymerization rates and selectivity using a systematic series of homoleptic Groups III–V metal alkoxide complexes, all d^0 configurations, reveals a metal structure-polymer linkage selectivity correlation. Plots of the polymer sequence selectivity (*ABB*) against the metal center Lewis acidity, as assessed by its hydrolysis constant (pK_h), show a linear correlation, identifying the most selective catalysts for bothpoly(ester-*alt*-ether) and polyester production. High Lewis acidity catalysts ($1 < pK_h < 0.6$) are best for poly(ester-*alt*-ethers) (*ABB*), while those with lower relative Lewis acidities ($8.1 < pK_h < 8.5$) are selective for polyesters (*AB*) and intermediate acidity metal catalysts form polymers with mixed linkages. The discovery of simple, commercial selective catalysts for epoxide and anhydride copolymerization is an important advance relevant to future production of elastomers, surfactants and adhesives.

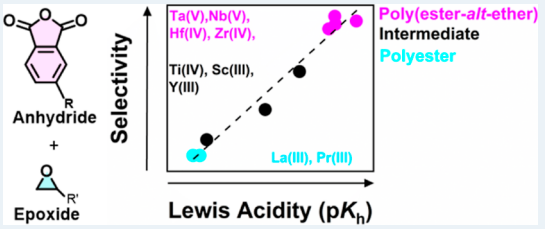

INTRODUCTION

Polyesters are high priority sustainable materials due to the biosourcing of many monomers, ability to tune structures to deliver in many applications, facility to undergo efficient, low-energy mechanical and chemical recycling and, in some cases, (bio)degradation.[1−9] Conventionally, polyesters are prepared by step-growth polymerization methods, but catalyzed chain-growth routes are desirable for the high atom economy, low temperatures, ability to control monomer sequences and compatibility with block polymer formation.[10,11]

The catalyzed ring opening copolymerization (ROCOP) of cyclic anhydrides (*A*) and epoxides (*B*) is such a controlled chain growth polymerization, useful to make aliphatic, semi-aromatic and functionalized polyesters featuring *AB* repeat units (Figure 1).[11−14] The best catalysts show high sequence selectivity, good control over molecular weights (M_n) and successfully enchain a wide range of epoxides and cyclic anhydrides.[11,14] Many epoxides and anhydrides are commercial products already used in industrial polymer manufacturing; some are already biosourced and others could become biosourced in future, which is important to help reduce embedded carbon dioxide emissions.[4] Another benefit of controlled *AB* (anhydride/epoxide) ROCOP is its use to make block polymers which show promise as thermoplastics and elastomers.[2,5,6] Current leading *AB* ROCOP metal-catalysts include multifunctional Cr(III), Co(III) or Al(III) complexes, incorporating ionic cocatalysts, or heterodinuclear Co(III)K(I), Fe(III)K(I), Al(III)K(I) or Zn(II)Mg(II) complexes.[11,14−25] Phosphazene bases, thio-ureas, amines and boranes, used in combination with each other and/or with ionic cocatalysts like phosphonium chlorides, are also effective catalysts.[26−31] These prior catalysts have been optimized for the formation of highly alternating *AB* polyesters, with >99% selectivity for ester repeat units now commonly observed.[11,14−25] Some of these catalysts are also effective in epoxide ring-opening polymerization (ROP), forming poly(ester-*b*-ethers) when using excess epoxide (vs anhydride) in the ROCOP.[10,11,14]

In 2022, we reported a Zr(IV) coordination complex, $[ZrL_2(O^iPr)_2]$, which exhibited a highly unusual selectivity in cyclic anhydride (*A*) and epoxide (*B*) ring-opening copolymerization (Figure 1).[32] It delivered poly(ester-*alt*-ethers) with very high (>95%) selectivity for *ABB* repeat units. In the

Received: December 2, 2025
Revised: February 16, 2026
Accepted: February 18, 2026
Published: March 3, 2026

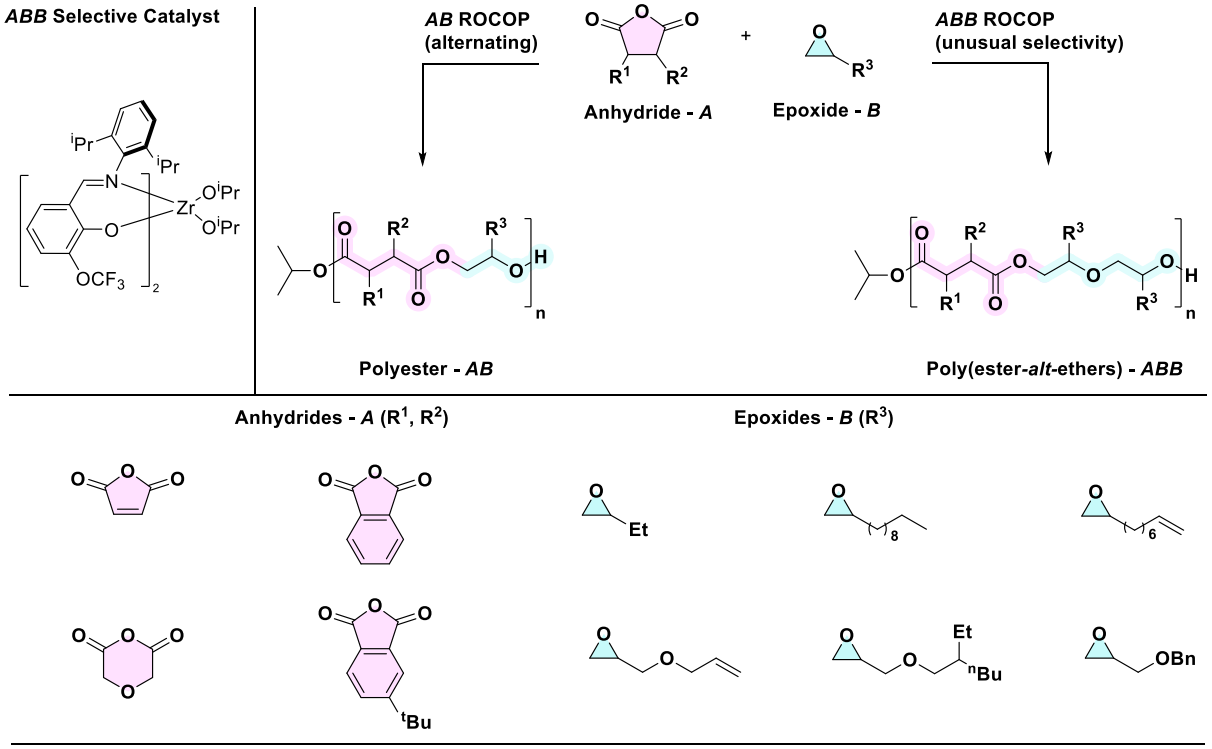

Figure 1. Poly(ester-*alt*-ether) ROCOP (*ABB*) of cyclic anhydrides (*A*) and epoxides (*B*) using the previously reported coordination complex Zr(IV) catalyst, $[ZrL_2(O^iPr)_2]$.[32] The catalyst, anhydrides and epoxides reported to produce polymers with *ABB* sequences are shown.[33,34]

Table 1. Ring-Opening Copolymerization (ROCOP) of Anhydride (tBuPA) and Epoxide (OO) Using Metal Alkoxides From Group III–V as Catalysts[a]

entry	catalyst	anhydride: epoxide degrees of polymerization (DP) [tBPA]/[OO][b,c]	poly(ester-*alt*-ether) selectivity (% *ABB* linkages)[d]	M_n (*Đ*) [kg mol^{-1}][e]	M_n (theo)[f] (# initiators)	k_{obs} ($\times 10^{-4}$ M s^{-1})[g]
1	$ZrL_2(O^iPr)_2$[32]	25:55	97	7.7 (1.16)	12.2 (2)	24 ± 0.4
2	$Zr(O^iPr)_4(HO^iPr)$	10:20	96	5.9 (1.25)	4.8 (5)	180 ± 10
3	$Zr(OEt)_4$	13:25	97	6.3 (1.23)	6.3 (4)	160 ± 6
4	$ZrCl_4$	13:27	95	5.3 (1.12)	5.9 (4)	200 ± 25
5	$Sc(O^iPr)_3$	17:24	39	7.7 (1.29)	6.6 (3)	10 ± 0.2
6	$Y(O^iPr)_3$	17:23	20	6.8 (1.45)	6.0 (3)	1 ± 0.3
7	$La(O^iPr)_3$	17:18	9	8.0 (1.28)	5.8 (3)	2 ± 0.01
8	$Pr(O^iPr)_3$	17:19	14	7.8 (1.29)	6.0 (3)	2 ± 0.01
9	$Ti(O^iPr)_4$	13:22	63	4.9 (1.25)	5.4 (4)	2 ± 0.2
10	$Zr(O^iPr)_4(HO^iPr)$	10:20	96	5.9 (1.25)	4.8 (5)	180 ± 10
11	$Hf(O^iPr)_4(HO^iPr)$	10:21	98	6.2 (1.28)	4.8 (5)	170 ± 12
12	$Nb(OEt)_5$	10:21	90	5.6 (1.23)	4.8 (5)	N.D.
13	$Ta(OEt)_5$	10:21	95	7.1 (1.28)	4.8 (5)	0.4 ± 0.02
14	$Zr(O^iPr)_4(HO^iPr)$[h]	10:19	82	4.1 (1.15)	4.0 (5)	N.D.
15	$Hf(O^iPr)_4(HO^iPr)$[h]	10:20	86	3.9 (1.15)	4.1 (5)	N.D.

[a]ROCOP conditions: [Cat] = 10 mM, [tBPA] = 0.5 M, OO = 1 mL, 120 °C, 40–360 s. [b]DP(tBuPA) was determined from the relative ratios of the integrals for the aromatic tBPA (7.91–8.01 ppm) vs P(tBPA) (7.34–7.84 ppm) resonances in the crude ^{1}H NMR spectra (Figures S8–S14). [c]DP(OO) was determined using the relative integrals for the aromatic (7.34–7.84 ppm) vs total ether and ester resonances (~3.2–5.5 ppm) in the crude polymer ^{1}H NMR spectra (Figures S8–S21). [d]Determined using the relative integrals for *AB* ester linkages (5.35 ppm) vs *ABB* ester-*alt*-ether linkages (5.10 ppm) (Figure S21). [e]Determined by gel permeation chromatography (GPC), using THF as the eluent, and calibrated using narrow MW polystyrene standards (Figure S22 and S24). [f]Theoretical M_n are calculated using monomer conversion data assuming that all alkoxide (and any alcohol) ligands initiate. [g]The rate coefficient is determined from linear fits to plots of [P(tBPA)] vs time, the errors are determined from repeat runs (Figure 2 and S23). [h]These reactions were open to air before polymerization (Figures S25–s28).

catalytic cycle, an anhydride insertion is followed by two sequential epoxide insertions (Figure 1).[32] The polymerization kinetics, investigated using phthalic anhydride, PA (*A*), and butylene oxide, BO (*B*), showed a rate law that is first order in each of epoxide (*B*) and catalyst concentrations, but zero order in anhydride (*A*) concentration (Figure S1).[32] The poly(ester-*alt*-ethers) were fully characterized, with the sequence selectivity confirmed by 1 and 2-D NMR spectroscopy, GPC, MALDI-ToF mass spectrometry and by complete ester linkage hydrolysis followed by HPLC-mass spectrometry analysis of the small-molecule products.[32,33] In 2024, the Zr(IV) catalyst showed very high *ABB* selectivity using other

https://doi.org/10.1021/acscatal.5c08568
ACS Catal. 2026, 16, 5673–5681

cyclic anhydrides and epoxides. The resulting poly(ester-*alt*-ethers) are amorphous elastomers with glass transition temperatures from −50 to 48 °C (Figure 1).[33] The Zr(IV) catalyst was also active in L-lactide ring opening polymerization.[34] Using a one-reactor process, it was used to make poly(ester-*alt*-ether)-*b*-(L-lactides) which were effective as fully recyclable, enzymatically degradable toughening for commercial poly(L-lactide) (Figure 1).[34] Our group and others have previously shown that some Sn(II) catalysts produced poly(ester-*ran*-ethers), but these catalysts lack the very high *ABB* linkage selectivity.[35−38] Poly(ester-*alt*-ethers) can also be produced by other controlled polymerizations, such as cyclic ester and epoxide terpolymerization or specialist lactone ring opening polymerizations; these reactions generally require rather specialist catalysts and/or custom synthesized monomers which prohibit widespread use.[39−43]

To apply the *ABB* selective catalysis, it is important to establish whether other metal complexes could behave equivalently to the Zr(IV) coordination complex. One limitation of the current Zr(IV) catalyst is that it needs to be synthesised and its isolated yield is rather low (∼20−25%). This arises because, although its ligand syntheses are straightforward, the complex is isolated by crystallization.[32,33] To investigate alternative catalysts, a series of commercial, homoleptic Zr(IV) complexes, featuring alkoxide or halide ligands (initiating groups), are selected. To understand whether other similar size and electronic configuration (d^0) metals would also be effective, a series of other commercial Group III−V metal alkoxide complexes are targeted, $M(OR)_n$·$(ROH)_m$, where M = Sc(III), Y(III), La(III), Pr(III), Ti(IV), Zr(IV), Hf(IV), Nb(V) or Ta(V) and R = Et or ^{i}Pr. The alkoxide ligands (OEt or O^{i}Pr) are likely to be effective polymerization initiators since they model one of the putative propagation intermediates, i.e. the metal alkoxide formed by epoxide ring-opening. The objective is to understand how these metals behave in catalysis, particularly in terms of poly(ester-*alt*-ether) (*ABB*) selectivity, polymerization rates (k_{obs}) and polymerization control.

RESULTS AND DISCUSSION

The homoleptic, Zr(IV) alkoxide and halide complexes were tested as catalysts with performances benchmarked against the previously reported catalyst, $[ZrL_2(O^iPr)_2]$. For these copolymerizations, *tert*-butyl phthalic anhydride (tBuPA) and octene oxide (OO) were used as monomers, due to the high solubility of all catalysts in them and their high boiling points, enabling higher reaction temperatures. All copolymerizations were conducted under common conditions, where [Zr]/[tBuPA]/[OO] = 1:50:660 at 120 °C (Table 1). The polymerization kinetics were assessed using a recently reported methodology, whereby rates are directly measured using a differential scanning calorimeter (DSC).[44] As an example of how this method was used under an inert atmosphere, $[Zr(O^iPr)_4(HO^iPr)]$ catalyst and monomers were added in the appropriate molar ratios to a DSC pan, which was heated rapidly to 120 °C and the copolymerization rates were analyzed from heat flow (W/g) vs time data, until complete anhydride consumption (Table 1 and Figure S2). The normalized heat flow (W/g) vs time (s) output was transformed into normalized anhydride (tBuPA) or P(tBuPA) concentration vs time data, using ^{1}H NMR spectroscopy to calibrate conversion (Figures S2 and S3).[44] In all cases, the normalized concentration of polymerized and initial anhydride concentrations are related by [P(tBuPA)] = 1-[tBuPA]. In the kinetic plots, the concentration of polymerized anhydride [P(tBuPA)] is used to measure the polymerization progress since regardless of the specific polymer sequence (which can vary), one anhydride is enchained in every repeat unit, i.e. sequences are either AB or ABB. In this work, the P(tBuPA) abbreviation is used to refer to the formation and concentration of polymer repeat units, regardless of the specific sequence, which is labeled ABB or AB selectivity. The P(tBuPA) should not be confused to mean that only anhydride is enchained in a repeat unit. The use of the label is important since it enables comparisons of activity to be drawn between all catalysts, regardless of their sequence selectivity. The kinetic plots show linear fits, over 10−80% P(tBuPA) conversions, with the rate coefficient (k_{obs}) as the gradient (Figure S3).[44] For all catalysts, the kinetic experiments were conducted in triplicate, with typical errors in rate coefficient values being <10%. To establish the accuracy of the DSC methodology, the same copolymerization ($[Zr(O^iPr)_4(HO^iPr)]$ as catalyst) was conducted with conventional aliquot analysis (Figures S2−S7).

Identical conditions were used, with the aliquots quenched at regular time intervals and the crude reaction products analyzed by ^{1}H NMR spectroscopy to determine the anhydride conversion (Figure S4). The polymerization rate coefficients are the same, within experimental errors, with k_{obs}(DSC) = 180 ± 10 × 10^{-4} M s^{-1} and k_{obs}(vial) = 163 × 10^{-4} M s^{-1} (Figures S3 and S4). Both the resulting polymers showed equivalent, very high *ABB* linkage selectivity: 96% for both DSC and aliquots (Figure S5). Both poly(ester-*alt*-ethers) show the same molar masses, as determined by GPC, with the DSC methodology yielding poly(ester-*alt*-ether) with M_n = 4.6 kg mol^{-1} ($Đ$ = 1.18) and the reaction aliquot method having M_n = 4.4 kg mol^{-1} ($Đ$ = 1.15) (Table 1 and Figure S6). Plots of molar mass (M_n) and dispersity ($Đ$) vs anhydride conversion show a linear increase in M_n and low dispersity values with increasing monomer conversion, consistent with the reaction being a well-controlled polymerization (Figure S7). Subsequently, all the new catalysts were investigated using the DSC method to measure rates, since it is fast, reliable and operates on a small-scale.

All the poly(ester-*alt*-ethers) were characterized using ^{1}H NMR spectroscopy to evaluate the polymer composition (*ABB* linkage selectivity), monomer conversion and relative degrees of polymerization (Figures S8−S21). In all cases, even though reactions occur in excess epoxide, there is no epoxide ROP or polyether formation after complete anhydride consumption, rather the excess epoxide remains unreacted once the anhydride is consumed (Figure S9). The conversion and degree of polymerization (DP) of the anhydride were determined using ^{1}H NMR spectroscopy by analysis of the relative integrals of the resonances assigned to tBuPA and P(tBuPA) (∼7.9 vs ∼7.5 ppm, respectively, Figures S8 and S20). The epoxide (OO) conversion, and hence degree of polymerization, was determined by comparing the relative P(tBuPA) resonances, against the sum of all the ring-opened epoxide linkages adjacent to ester and ether groups (∼3.2−5.5 ppm) (Figures S8 and S21). The poly(ester-*alt*-ether) selectivity ([*AB*]/[*ABB*]) was determined by comparing the integrals of the methine ester resonances, since these signals occur at different chemical shifts for *AB* polyesters (5.35 ppm) compared with *ABB* poly(ester-*alt*-ethers) (5.10 ppm, Figures S21).

https://doi.org/10.1021/acscatal.5c08568
ACS Catal. 2026, 16, 5673−5681

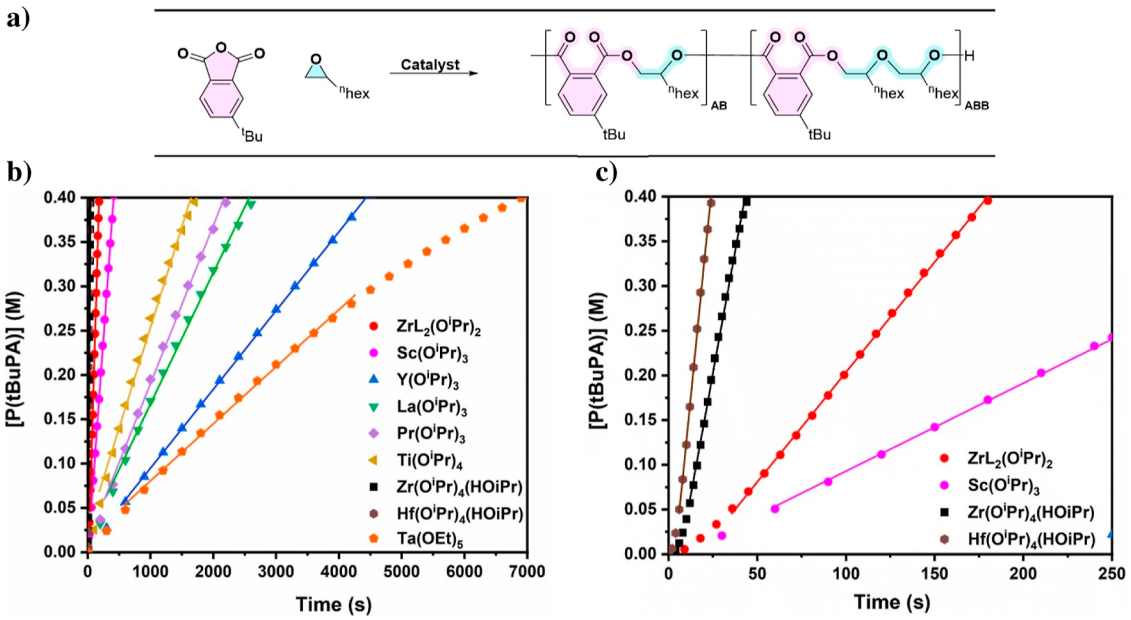

Figure 2. Kinetic data for the metal alkoxide catalysts, using metals from groups III–V. Plots of [P(tBuPA)] vs time for the series of $M(OR)_n{\cdot}(HOR)_m$ catalysts. (a) Anhydride and epoxide ROCOP; conditions: $[M(OR)_n{\cdot}(HOR)_m]/[tBuPA]/[OO]$ = 1:50:654, 1 mL OO, 120 °C (Table 1). (b) Plot of [P(tBuPA)] vs time for all catalysts, with linear fits included (Figures S2 and S3). The pseudo rate coefficients, k_{obs} ($M\ s^{-1}$) are the gradients of the linear fits (from 10 to 80% conversion, except $Ta(OEt)_5$ which was fit between 10 and 60%). (c) Plot for the fastest catalysts: $(Zr(O^iPr)_4(HO^iPr)$, $Hf(O^iPr)_4(O^iPr)$, $Sc(O^iPr)_3$ and $ZrL_2(O^iPr)_2$. All kinetic data show $R^2 > 0.99$.

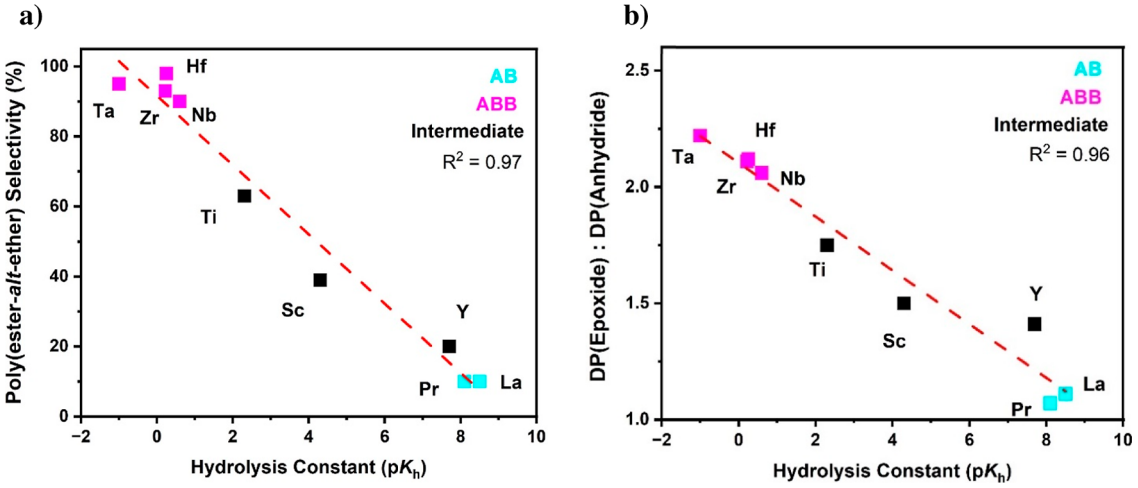

Figure 3. Relationship between the hydrolysis constant (pK_h)[45,47] and (a) the selectivity for poly(ester-*alt*-ether) and (b) the epoxide equivalents enchained per anhydride (DP(epoxide)/DP(anhydride)) by d^0 alkoxides $(M(OR)_n(HOR)_m)$. Note that DP(epoxide)/DP(anhydride) ~2 for selective poly(ester-*alt*-ether) linkage incorporation (Zr(IV), Hf(IV), Ta(V), Nb(V)), and, = 1 for polyester (La(III), Pr(III)). See Table S1 for further details on pK_h values.

The $Zr(IV)X_4$ catalysts, where X = $(O^iPr)_2(HO^iPr)$, OEt, Cl, were compared against the known *ABB* selective catalyst $[ZrL_2(O^iPr)_2]$ (Table 1).The homoleptic Zr(IV) catalysts all showed high rates, with $160 \pm 6 \times 10^{-4} < k_{obs} < 200 \pm 25 \times 10^{-4}$ $M\ s^{-1}$ and ≥95% poly(ester-*alt*-ether) selectivity (Table 1). The resulting poly(ester-*alt*-ethers) have M_n = 4.6–6.3 kg mol^{-1} with monomodal molar mass distributions and narrow dispersity, $1.12 < Đ < 1.23$ (Table 1 and Figure S22). Comparing the experimental and theoretical molar mass values suggests that all ligands, and, any free alcohol, function as initiators. The catalysts are fast, highly selective, and well controlled: their rates, at equivalent Zr(IV) concentrations, are ~8× times faster than the $[ZrL_2(O^iPr)_2]$ catalyst (Table 1 and Figures S23). The key finding is that the ancillary ligand (L) is not necessary for fast poly(ester-*alt*-ether) catalysis.

Next, metal alkoxide complexes with the same d^0 electronic configuration were applied using metals from groups III–V (and praseodymium): $Sc(O^iPr)_3$, $Y(O^iPr)_3$, $La(O^iPr)_3$, $Pr(O^iPr)_3$, $Ti(O^iPr)_4$, $Zr(O^iPr)_4(HO^iPr)$, $Hf(O^iPr)_4(O^iPr)$, $Nb(OEt)_5$ and $Ta(OEt)_5$. All the complexes were active but showed variable rates, with k_{obs} values from 0.4 ± 0.02 to $180 \pm 10 \times 10^{-4}$ $M\ s^{-1}$ and *ABB* sequence selectivity values from ~10 to >95% (Table 1, Figures 2 and S21). The polymers' $M_{n,GPC}$ values suggest that all the alkoxide (and alcohol) ligands initiate the polymerizations (Table 1 and Figure S24). The fastest and most selective catalysts are the Zr(IV) and

https://doi.org/10.1021/acscatal.5c08568
ACS Catal. 2026, 16, 5673–5681

Hf(IV) alkoxides, with all the other metals showing slower polymerizations (Table 1 and Figure 2).

The Zr(IV), Hf(IV), Nb(V) and Ta(V) alkoxides all produced polymers with almost quantitative *ABB* linkage selectivity, i.e. poly(ester-*alt*-ethers). On the other hand, the Y(III), La(III) and Pr(III) complexes produced polyesters with high or very high selectivity for *AB* linkages, i.e. polyesters. The Ti(IV) and Sc(III) alkoxides produced polymers showing an approximately even distribution of *AB* (ester) and *ABB* (ester-*alt*-ether) linkages. In the latter case, DOSY NMR spectroscopy showed that all resonances have the same diffusion rate, which suggests a random ester and ester-*alt*-ether linkage selectivity in each polymer chain, rather than formation of mixtures of polymers (Figures S29−S31).

The relationship between the metal centers and monomer selectivity was explored by plotting *ABB* selectivity vs known metal center physical parameters, including M(III−V) ionic radius, M-OR bond lengths or metal Lewis acidity (metal ion hydrolysis constant pK_h, Figures 3a, S32−S35 and Table S1).[45,46]

The plot of *ABB* selectivity vs metal ionic radii, assuming hexacoordinate geometries, is very scattered and could not be effectively fit (r^2 = 0.68, Figure S32 and Table S1).[46] The lack of any obvious correlation between catalytic selectivity and metal ionic radius is apparent when comparing the most effective catalysts Zr(IV) and Hf(IV) (r = 0.71 Å) which have >95% *ABB* selectivity, with the similar ionic radius Sc(III) catalyst (r = 0.75 Å) which shows just 40% selectivity (Tables 1, S1 and Figure S32). Also, the Ta(V) catalyst (r = 0.61 Å) is 95% *ABB* selective, while the similarly sized Ti(IV) catalyst (r = 0.6 Å) shows an *ABB* selectivity of just 63% (Tables 1, S1 and Figure S32). One advantage of using these known, simple homoleptic metal alkoxide catalysts is that many of their solid-state structures are characterized using single crystal X-ray diffraction. In the solid state, these complexes often form dimers and multinuclear clusters (Table S1 and Figure S33). Plots comparing the *ABB* selectivity vs M-OR bond lengths, using data for both bridging and terminal alkoxide bonds, did not show any obvious linear fits (Figures S34, S35 and Table S1). The only generalization is that most selective catalysts tend to show intermediate ionic radii and M-OR bond lengths, i.e. 0.64 ≤ metal ionic radii ≤ 0.72 Å, 1.90 ≤ terminal M-OR ≤ 1.94 Å (Table S1 and Figures S33−S35). In contrast, plotting the *ABB* linkage selectivity against the metal Lewis acidity, as assessed by its hydrolysis constant, pK_h, shows a clear linear fit (Figure 3, r^2 = 0.97).[45] In the plot, high selectivity (>90%) values correlate with poly(ester-*alt*-ether) production, while very low values (0−10%) correlate with alternating polyester production (Figure 3). The linear fit shows that the metal Lewis acidity relates directly to the type of product formed: metals with low pK_h values, i.e. −1 < pK_h < 0.6, select for *ABB* linkages, e.g. Zr(IV), Hf(IV), Nb(V) or Ta(V). Metals showing higher pK_h values, i.e. 8.1 < pK_h < 8.5, select for *AB* linkages, e.g. La(III) or Pr(III). Metals with intermediate pK_h values, i.e. 2.3 < pK_h < 4.3, produce random sequence enchainment and mixtures of ester and ester-ether linkages, e.g. Sc(III) or Ti(IV) (Figure 3a). Plotting the DP(anhydride)/DP(epoxide) vs metal pK_h values shows exactly the same trends and linear fit (Figure 3b).

The use of hydrolysis constant values as a measure for metal Lewis acidity warrants discussion, particularly since the polymerizations are all conducted anhydrously.[48] Metal hydrolysis constants are known to correlate directly to the metal Lewis acidity values and it is the latter which are appropriate to understand catalytic performances for these reactions.[48] The hydrolysis constant data are useful since they are all measured on a common scale, applicable to many metals.[48] In contrast there is no such common scale for Lewis acidity and its measurement tends to be indirect, relying on insensitive NMR titrations.[48] Other researchers in fields spanning electrocatalysis, organic asymmetric catalysis and polymerizations have all reported upon the utility of Bronsted acidity values (pK_a or pK_h) to inform upon the metal Lewis acidity.[48−54] In these areas of catalysis, metal ion pK_h values have proven effective to understand linear free energy relationships for reactions conducted under anhydrous conditions.[48−56] For example, Shibasaki and co-workers applied metal ion hydrolysis constants to rationalize performances of Lewis acidic metal catalysts for aziridine ring-opening reactions.[48,57−60] Mashima, Okuda, Nozaki and co-workers investigated lanthanide/Zn(II) heterotetranuclear catalysts for carbon dioxide/epoxide ROCOP showing a weak correlation between catalytic activity and lanthanide Lewis acidity (as assessed by metal ion pK_h).[48,55,56] In our work developing heterodinuclear M(III)M′(I) catalysts for CO_2/epoxide and epoxide/anhydride ROCOP (*AB*-selective), we showed linear free energy (exponential) relationships between rate and s-block metal (M′) pK_a values.[22,51,52] In prior work, metal ion hydrolysis constants were correlated to catalytic activity;[48] here, in contrast, the correlation is with the polymerization selectivity and, therefore, the resulting polymer sequence. This means the relative metal-alkoxide Lewis acidity controls the monomer selectivity either by reaction with an epoxide or anhydride: such selectivity is very unusual and the insights provided by the Lewis acidity correlation should help to understand both how and why poly(ester-*alt*-ethers) form.[32] Qualitatively, the metal active site Lewis acidity is implicated in both epoxide activation and insertion processes. The structure−selectivity relationships suggest that the transition state energy differences between the metal-alkoxide intermediate reacting with another epoxide or with an anhydride correlate with the metal Lewis acidity values; future in depth mechanistic investigations are, of course, necessary and ongoing.

The ability to use commercial catalysts and rationalize their selectivity using the Lewis acidity correlation should facilitate uptake of the catalysis by polymer chemists seeking to make and investigate new materials. The correlation data also helps understand why *ABB* selective reactions were not previously discovered. Prior research into epoxide/anhydride ROCOP catalysts focused in quite a different region of relative metal Lewis acidity, e.g. Cr(III) (pK_h = 4.0), Co(III) (pK_h = 3), Zn(II) (pK_h = 9.0), Na(I) (pK_h = 14.2), K(I) (pK_h = 14.5) or Al(III) (pK_h = 3−5).[11,14−25,45,47] Most of these metals have considerably lower Lewis acidity (higher pK_h) than the Group III−V metals that select for ester-*alt*-ether enchainment. The most selective *ABB* catalysts are strong Lewis acids, with −1 < pK_h < 0.6.

Another aspect is that prior investigations of Group III−V catalysts always applied ionic cocatalysts, such as bis(triphenylphosphine)iminium chloride PPNCl.[61−66] In these catalyst systems, metal-ate complexes are likely to form, which are substantially less Lewis acidic, and the ROCOP selectivity reverts to the more common *AB* polyester production.[61−65] For example, Fieser and co-workers developed a YCl_3/PPNCl catalyst system showing high *AB* linkage selectivity for different

https://doi.org/10.1021/acscatal.5c08568
ACS Catal. 2026, 16, 5673−5681

anhydride and epoxide combinations.[61,62,66] Kozak and co-workers used Schiff base Zr(IV) alkoxide/PPNCl catalysts which showed high-selectivity for *AB*-polyesters.[63] Other Schiff base Ti(IV)/PPNCl and Zr(IV)/PPNCl catalysts also showed highly selective *AB* polyester formation.[64] Future catalyst development for poly(ester-*alt*-ether), *ABB* selectivity, should avoid ionic cocatalysts and rather fine-tune metal Lewis acidity by using ancillary ligands.

Overall, the homoleptic Zr(IV), Hf(IV) and Ta(V) alkoxide complexes are very selective catalysts for poly(ester-*alt*-ethers) (*ABB* polymers). These catalysts are attractive as they are commercial and simple to use. For the two lead catalysts, we investigated the need for anaerobic handling. Polymerizations applying $Zr(O^iPr)_4(HO^iPr)$ or $Hf(O^iPr)_4(HO^iPr)$ as catalysts ([Cat] = 10 mM, [tBPA] = 0.5 M, OO = 1 mL, 120 °C) were conducted after the starting catalyst solution was left open to air (Table 1). In the resulting epoxide/anhydride copolymerizations, there was some reduction in poly(ester-*alt*-ether) selectivity, to 82 and 86% for Zr(IV) and Hf(IV) catalysts, respectively (Figures S25−S28). Nonetheless, the polymerizations remained well-controlled, with the molar mass values, by GPC, matching theoretical values quite closely (Figures S26 and S28).

The linkage selectivity also provides a means to tune the polymer physical properties, such as the glass transition temperature. Catalysts spanning the selectivity range were used to prepare polymers with the same overall degree of polymerization of the anhydride (DP = 20, Table S2 and Figures S29−S31). As such, the La(III) catalyst formed an alternating polyester (*AB* = 91%, *ABB* = 9%), the Sc(III) catalyst formed a polymer with mixtures of ester and ester-ether linkages (*AB* = 51%, *ABB* = 49%), the Ti(IV) catalyst also formed mixtures of linkages but with a bias of 77% *ABB* (ester-*alt*-ether) and the Hf(IV) catalyst formed only poly(ester-*alt*-ethers) with >99% *ABB* linkage selectivity (Table S2). All the polymers are amorphous and show only glass transition temperatures. Further, as the proportion of ether linkages increases, from *AB* to *ABB* sequences, so the polymers' glass transition temperatures decrease, consistent with enhanced segmental motion afforded by the ether linkages (Figure S36a and Table S2).[32,33] For example, the alternating *AB* polyester (La(III) catalyst) shows a T_g value of 4 °C while the *ABB* poly(ester-*alt*-ether) (Hf(IV) catalyst) shows a lower T_g value of −17 °C, with intermediary values for those with mixed linkages (Figure S36a). For all the polymers, the on-set of thermal decomposition temperature ($T_{d,5\%}$) remained relatively high at 294−309 °C, providing the materials with a wide processing temperature window (Table S2 and Figure S36b).

METHODS

Materials

The synthesis of the previously reported catalyst $[ZrL_2(O^iPr)_2]$, monomer purifications, and polymerizations were carried out under inert conditions, using standard Schlenk techniques and in a N_2-filled glovebox. The catalyst $[ZrL_2(O^iPr)_2]$ was synthesized using literature procedures.[32] Octene oxide (OO) was dried by stirring over CaH_2, followed by fractional distillation. It was then dried (over BuLi), followed by two further fractional distillations. 3-*tert*-Butyl-phthalic anhydride (tBPA) was purified by sublimation (three times). All monomers were stored under an inert (N_2) atmosphere. $Zr(O^iPr)_4(HO^iPr)$, $Hf(O^iPr)_4(HO^iPr)$, $Y(O^iPr)_3$, $Ta(OEt)_5$, $Pr(O^iPr)_3$ and $Zr(OEt)_4$ were purchased from STREM chemicals. $Ta(OEt)_5$ was purchased from Thermo Scientific Chemicals. $Sc(O^iPr)_3$ was purchased from Santa Cruz Biotechnology. $Ti(O^iPr)_4$, $La(O^iPr)_3$, $Zr(Cl)_4$ and $Nb(OEt)_5$ purchased from Sigma-Aldrich. Catalysts were used as purchased.

NMR Spectroscopy

^1H and COSY NMR spectra were obtained using Bruker AV 400 MHz, 500 and 600 MHz instruments. ^1H DOSY spectra were obtained using a Bruker NEO600 NMR spectrometer. NMR spectra are shown in the Supporting Information (Figures S5, S8−21, S25, S27, S29−S31).

Gel Permeation Chromatography (GPC)

Polymer analysis was carried out using a Shimadzu LC-20AD instrument, equipped with PSS SDV 5 μm precolumn and two PSS SDV 5 μm linear M columns and a Refractive Index (RI) detector. Samples were dissolved in HPLC grade THF, filtered through 0.2 μm PTFE filters (VWR) and measurements were determined at 1 mL min^{-1} flow rate, at 30 °C. Monodisperse polystyrene standards were used to calibrate the instrument. GPC data are presented in Figures S6, S22, S24, S26 and S28.

Differential Scanning Calorimetry (DSC)

Thermal analyses were conducted using the DSC25 instrument (TA Instruments). A sealed, empty crucible was used as a reference, and the instrument was calibrated using zinc and indium samples. Polymer samples were heated from −80 to 150 °C, at a rate of 10 °C min^{-1} and under a N_2 flow (80 mL min^{-1}). Samples were subsequently cooled to −80 °C, at a rate of 10 °C min^{-1}, and kept at −80 °C for a further 5 min, followed by a heating−cooling cycle from −80 to 150 °C, at a rate of 10 °C min^{-1}. Each sample was analyzed over two heating−cooling cycles. Glass transition temperatures (T_g) are reported as the midpoint of the transition taken from the second heating cycle. Data are presented in Figure S36.

Thermal Gravimetric Analysis (TGA)

Sample high temperature stability was measured using a TGA5500 system (TA Instruments) equipped with the TRIOS software package. Polymer samples were heated from 40 to 700 °C, at a rate of 10 °C min^{-1}, under N_2 flow (12 mL min^{-1}). Data are presented in Figure S36.

Polymerization Kinetics

Generally, kinetics experiments were conducted using a DSC instrument using methods which were previously described for epoxide/anhydride ROCOP and, to calibrate the method, some vial kinetics were also conducted (Figures S2−S4).[44] In the DSC method, the catalyst (0.01 mol) was weighed into a vial, then dissolved in octene oxide (1 mL, such that [cat]/[tBPA]/[OO] = 1:50:654). 3-*tert*-Butyl phthalic anhydride (0.5 mmol) was added to the reaction mixture until fully dissolved. Next, a ∼10 mg sample was transferred to a preweighed DSC pan which was sealed and weighed. Samples were analyzed at 120 °C using a methodology where the DSC instrument was rapidly heated to 120 °C and then the reference and sample pans were automatically loaded into the instrument. All measurements were carried out using sealed pans (unless otherwise stated), under N_2 flow (50 mL min^{-1}). The normalized heat flow (W/g) vs time (s) data was integrated, using the Trios software (v5.7.1.74) with the kinetics add-on package (Figure S2). Once the reaction was complete, the crude sample was also analyzed by NMR spectroscopy and GPC. The ^1H NMR spectrum was used to determine the anhydride conversion for subsequent use in the kinetic plots (concentration vs time, Figures S2−S4, S8−S21). It was also used to determine the polymerization selectivity, using methods which were previously reported (Figures S5).[32,33] GPC data were used to determine the polymer molar mass and dispersity (Figures S6, S22, S24, S26 and S28). The DSC kinetics experiments were conducted in triplicate for error analysis.

https://doi.org/10.1021/acscatal.5c08568
ACS Catal. 2026, 16, 5673−5681

CONCLUSIONS

Overall, commercial Zr(IV), Hf(IV) and Ta(V) alkoxide catalysts combine high rates, good polymerization control and very high ester-*alt*-ether linkage selectivity in the copolymerizations of cyclic anhydride and epoxide. Comparing the catalytic selectivity across a systematic series of metal alkoxides, where metals are from groups III−V, catalysts shows a clear linear correlation between the linkage selectivity and the metal Lewis acidity, as assessed through its hydrolysis constant (pK_h). Metals showing high Lewis acidity ($-1 < pK_h < 0.6$) are very selective for ester-*alt*-ether linkages, while those with lower Lewis acidity ($8.1 < pK_h < 8.5$) favor ester linkages and catalysts with intermediate acidity ($2.3 < pK_h < 4.3$) produce polymers with mixtures of both linkages. The use of commercial metal alkoxide catalysts provides a straightforward future route to make and study these new types of sustainable polymers and should accelerate application development as degradable surfactants, debondable adhesives and ion conducting polyelectrolytes, as well as for recyclable plastics and elastomers.

ASSOCIATED CONTENT

Supporting Information

The open-access experimental data-sets which support this publication can be found via the DOI 10.5287/ora-avbnbdz7y. The Supporting Information is available free of charge at https://pubs.acs.org/doi/10.1021/acscatal.5c08568.

Supporting information experimental materials and methods, catalysis protocols, proposed catalytic cycle, DSC polymerization kinetics data, polymerization selectivity data, polymer GPC data, catalysis and polymer characterization data for all polymers, data for quantified structure−selectivity relationships ionic radii, M-OR bond lengths, hydrolysis constant data, polymer T_g and TGA data (PDF)

AUTHOR INFORMATION

Corresponding Author

Charlotte K. Williams − *Department of Chemistry, Chemistry Research Laboratory, University of Oxford, Oxford OX1 3TA, U.K.*; orcid.org/0000-0002-0734-1575; Email: Charlotte.williams@chem.ox.ac.uk

Authors

Ryan W. F. Kerr − *Department of Chemistry, Chemistry Research Laboratory, University of Oxford, Oxford OX1 3TA, U.K.*

Alexander R. Craze − *Department of Chemistry, Chemistry Research Laboratory, University of Oxford, Oxford OX1 3TA, U.K.*

Complete contact information is available at: https://pubs.acs.org/10.1021/acscatal.5c08568

Notes

The authors declare no competing financial interest.

ACKNOWLEDGMENTS

The EPSRC (EP/S018603/1), EPSRC Sustainable Chemicals and Materials Manufacturing Hub (EP/Z532782/1) and EPSRC UK Catalysis Hub (UKRI945) are acknowledged for research funding.

REFERENCES

(1) Cywar, R. M.; Rorrer, N. A.; Hoyt, C. B.; Beckham, G. T.; Chen, E. Y. X. Bio-based polymers with performance-advantaged properties. *Nat. Rev. Mater.* **2022**, *7* (2), 83−103.

(2) Payne, J.; Jones, M. D. The Chemical Recycling of Polyesters for a Circular Plastics Economy: Challenges and Emerging Opportunities. *ChemSusChem* **2021**, *14* (19), 4041−4070.

(3) Coates, G. W.; Getzler, Y. D. Y. L. Chemical recycling to monomer for an ideal, circular polymer economy. *Nat. Rev. Mater.* **2020**, *5* (7), 501−516.

(4) Zhou, L.; Zhang, Z.; Shi, C.; Scoti, M.; Barange, D. K.; Gowda, R. R.; Chen, E. Y.-X. Chemically circular, mechanically tough, and melt-processable polyhydroxyalkanoates. *Science* **2023**, *380* (6640), 64−69.

(5) Häußler, M.; Eck, M.; Rothauer, D.; Mecking, S. Closed-loop recycling of polyethylene-like materials. *Nature* **2021**, *590* (7846), 423−427.

(6) Desveaux, J. S.; Uekert, T.; Curley, J. B.; Choi, H.; Liang, Y. Z.; Singh, A.; Mante, O. D.; Beckham, G. T.; Jacobsen, A. J.; Knauer, K. M. Mixed polyester recycling can enable a circular plastic economy with environmental benefits. *One Earth* **2024**, *7* (12), 2204.

(7) Zhang, Z.; Quinn, E. C.; Kenny, J. K.; Grigoropoulos, A.; DesVeaux, J. S.; Chen, T.; Zhou, L.; Xu, T.; Beckham, G. T.; Chen, E. Y.-X. Stereomicrostructure-regulated biodegradable adhesives. *Science* **2025**, *387* (6731), 297−303.

(8) Vidal, F.; van der Marel, E. R.; Kerr, R. W. F.; McElroy, C.; Schroeder, N.; Mitchell, C.; Rosetto, G.; Chen, T. T. D.; Bailey, R. M.; Hepburn, C.; et al. Designing a circular carbon and plastics economy for a sustainable future. *Nature* **2024**, *626* (7997), 45−57.

(9) Aarsen, C. V.; Liguori, A.; Mattsson, R.; Sipponen, M. H.; Hakkarainen, M. Designed to Degrade: Tailoring Polyesters for Circularity. *Chem. Rev.* **2024**, *124* (13), 8473−8515.

(10) Zhang, X.; Fevre, M.; Jones, G. O.; Waymouth, R. M. Catalysis as an Enabling Science for Sustainable Polymers. *Chem. Rev.* **2018**, *118* (2), 839−885.

(11) Lidston, C. A. L.; Severson, S. M.; Abel, B. A.; Coates, G. W. Multifunctional Catalysts for Ring-Opening Copolymerizations. *ACS Catal.* **2022**, *12* (18), 11037−11070.

(12) Diment, W. T.; Lindeboom, W.; Fiorentini, F.; Deacy, A. C.; Williams, C. K. Synergic Heterodinuclear Catalysts for the Ring-Opening Copolymerization (ROCOP) of Epoxides, Carbon Dioxide, and Anhydrides. *Acc. Chem. Res.* **2022**, *55* (15), 1997−2010.

(13) Longo, J. M.; Sanford, M. J.; Coates, G. W. Ring-Opening Copolymerization of Epoxides and Cyclic Anhydrides with Discrete Metal Complexes: Structure-Property Relationships. *Chem. Rev.* **2016**, *116* (24), 15167−15197.

(14) Paul, S.; Zhu, Y.; Romain, C.; Brooks, R.; Saini, P. K.; Williams, C. K. Ring-opening copolymerization (ROCOP): synthesis and properties of polyesters and polycarbonates. *Chem. Commun.* **2015**, *51* (30), 6459−6479.

(15) Lidston, C. A. L.; Abel, B. A.; Coates, G. W. Bifunctional Catalysis Prevents Inhibition in Reversible-Deactivation Ring-Opening Copolymerizations of Epoxides and Cyclic Anhydrides. *J. Am. Chem. Soc.* **2020**, *142* (47), 20161−20169.

(16) Xia, X.; Suzuki, R.; Takojima, K.; Jiang, D.-H.; Isono, T.; Satoh, T. Smart Access to Sequentially and Architecturally Controlled Block Polymers via a Simple Catalytic Polymerization System. *ACS Catal.* **2021**, *11* (10), 5999−6009.

(17) Li, J.; Liu, Y.; Ren, W.-M.; Lu, X.-B. Asymmetric Alternating Copolymerization of Meso-epoxides and Cyclic Anhydrides: Efficient Access to Enantiopure Polyesters. *J. Am. Chem. Soc.* **2016**, *138* (36), 11493−11496.

(18) Abel, B. A.; Lidston, C. A. L.; Coates, G. W. Mechanism-Inspired Design of Bifunctional Catalysts for the Alternating Ring-Opening Copolymerization of Epoxides and Cyclic Anhydrides. *J. Am. Chem. Soc.* **2019**, *141* (32), 12760−12769.

(19) Li, Y.-N.; Liu, Y.; Yang, H.-H.; Zhang, W.-F.; Lu, X.-B. Intramolecular Partners in Asymmetric Catalysis Copolymerization: Highly Enantioselective and Controllable at Enhanced Temperatures

and Low Loadings. *Angew. Chem., Int. Ed.* **2022**, *61* (22), No. e202202585.
(20) Cui, L.; Ren, B.-H.; Lu, X.-B. Trinuclear salphen−chromium(III)chloride complexes as catalysts for the alternating copolymerization of epoxides and cyclic anhydrides. *J. Polym. Sci.* **2021**, *59* (16), 1821−1828.
(21) Diment, W. T.; Gregory, G. L.; Kerr, R. W. F.; Phanopoulos, A.; Buchard, A.; Williams, C. K. Catalytic Synergy Using Al(III) and Group 1 Metals to Accelerate Epoxide and Anhydride Ring-Opening Copolymerizations. *ACS Catal.* **2021**, *11* (20), 12532−12542.
(22) Fiorentini, F.; Eisenhardt, K. H. S.; Deacy, A. C.; Williams, C. K. Synergic Catalysis: the Importance of Intermetallic Separation in Co(III)K(I) Catalysts for Ring Opening Copolymerizations. *J. Am. Chem. Soc.* **2024**, *146* (33), 23517−23528.
(23) Jeon, J. Y.; Eo, S. C.; Varghese, J. K.; Lee, B. Y. Copolymerization and terpolymerization of carbon dioxide/propylene oxide/phthalic anhydride using a (salen)Co(III) complex tethering four quaternary ammonium salts. *Beilstein J. Org. Chem.* **2014**, *10*, 1787−1795.
(24) Diment, W. T.; Rosetto, G.; Ezaz-Nikpay, N.; Kerr, R. W. F.; Williams, C. K. A highly active, thermally robust iron(iii)/potassium(i) heterodinuclear catalyst for bio-derived epoxide/anhydride ring-opening copolymerizations. *Green Chem.* **2023**, *25* (6), 2262−2267.
(25) Reis, N. V.; Deacy, A. C.; Rosetto, G.; Durr, C. B.; Williams, C. K. Heterodinuclear Mg(II)M(II) (M = Cr, Mn, Fe, Co, Ni, Cu and Zn) Complexes for the Ring Opening Copolymerization of Carbon Dioxide/Epoxide and Anhydride/Epoxide. *Chem.—Eur. J.* **2022**, *28* (14), No. e202104198.
(26) Zhang, J.; Wang, L.; Liu, S.; Li, Z. Phosphazene/Lewis Acids as Highly Efficient Cooperative Catalyst for Synthesis of High-Molecular-Weight Polyesters by Ring-Opening Alternating Copolymerization of Epoxide and Anhydride. *J. Polym. Sci.* **2020**, *58* (6), 803−810.
(27) Xie, Z.; Yang, Z.; Hu, C.; Bai, F.-Q.; Li, N.; Wang, Z.; Ku, S.; Pang, X.; Chen, X.; Wang, X. Record-High-Molecular-Weight Polyesters from Ring-Opening Copolymerization of Epoxides and Cyclic Anhydrides Catalyzed by Hydrogen-Bond-Functionalized Imidazoles. *J. Am. Chem. Soc.* **2025**, *147* (14), 12115−12126.
(28) Zhang, Y.-Y.; Yang, G.-W.; Xie, R.; Zhu, X.-F.; Wu, G.-P. Sequence-Reversible Construction of Oxygen-Rich Block Copolymers from Epoxide Mixtures by Organoboron Catalysts. *J. Am. Chem. Soc.* **2022**, *144* (43), 19896−19909.
(29) Ji, H.-Y.; Wang, B.; Pan, L.; Li, Y.-S. Lewis pairs for ring-opening alternating copolymerization of cyclic anhydrides and epoxides. *Green Chem.* **2018**, *20* (3), 641−648.
(30) Clark, E. F.; Dunstan, E.; Kociok-Köhn, G.; Buchard, A. Aminophosphonium organocatalysts for the ring-opening copolymerisation of epoxide and cyclic anhydride. *Chem. Commun.* **2024**, *60* (89), 13067−13070.
(31) Xie, R.; Zhang, Y.-Y.; Yang, G.-W.; Zhu, X.-F.; Li, B.; Wu, G.-P. Record Productivity and Unprecedented Molecular Weight for Ring-Opening Copolymerization of Epoxides and Cyclic Anhydrides Enabled by Organoboron Catalysts. *Angew. Chem., Int. Ed.* **2021**, *60* (35), 19253−19261.
(32) Kerr, R. W. F.; Williams, C. K. Zr(IV) Catalyst for the Ring-Opening Copolymerization of Anhydrides (A) with Epoxides (B), Oxetane (B), and Tetrahydrofurans (C) to Make ABB- and/or ABC-Poly(ester-alt-ethers). *J. Am. Chem. Soc.* **2022**, *144* (15), 6882−6893.
(33) Kerr, R. W. F.; Craze, A. R.; Williams, C. K. Cyclic ether and anhydride ring opening copolymerisation delivering new ABB sequences in poly(ester-alt-ethers). *Chem. Sci.* **2024**, *15* (29), 11617−11625.
(34) Craze, A. R.; Kerr, R. W. F.; McGuire, T. M.; Wille, L.; Williams, C. K. Toughened commercial poly(l-lactide) (PLLA) using degradable and recyclable poly(ester-alt-ether)-b-PLLA. *Green Chem.* **2025**, *27* (31), 9495−9511.
(35) Quek, T.; Chumsaeng, P.; Phomphrai, K. Heteroleptic phenoxyimino tin(ii) bis(trimethylsilyl)amides for the synthesis of poly(diester-ethers) from cyclohexene oxide and succinic anhydride. *Dalton Trans.* **2025**, *54* (12), 5143−5152.
(36) Yuntawattana, N.; Gregory, G. L.; Carrodeguas, L. P.; Williams, C. K. Switchable Polymerization Catalysis Using a Tin(II) Catalyst and Commercial Monomers to Toughen Poly(l-lactide). *ACS Macro Lett.* **2021**, *10* (7), 774−779.
(37) Jabprakon, N.; Chumsaeng, P.; Phomphrai, K. Synthesis of ABx and ABxC poly(ester-ether) polymers: polymer sequences and effects of Bx and BxC units on thermal properties. *Polym. Chem.* **2023**, *14* (36), 4169−4181.
(38) Ungpittagul, T.; Jaenjai, T.; Roongcharoen, T.; Namuangruk, S.; Phomphrai, K. Unprecedented Double Insertion of Cyclohexene Oxide in Ring-Opening Copolymerization with Cyclic Anhydrides Catalyzed by a Tin(II) Alkoxide Complex. *Macromolecules* **2020**, *53* (22), 9869−9877.
(39) Uenishi, K.; Sudo, A.; Endo, T. Anionic Alternating Copolymerizability of Epoxide and 3,4-Dihydrocoumarin by Imidazole. *Macromolecules* **2007**, *40* (18), 6535−6539.
(40) Fan, H.-Z.; Yang, X.; Wu, Y.-C.; Cao, Q.; Cai, Z.; Zhu, J.-B. Leveraging the monomer structure for high-performance chemically recyclable semiaromatic polyesters. *Polym. Chem.* **2023**, *14* (6), 747−753.
(41) Libiszowski, J.; Kowalski, A.; Szymanski, R.; Duda, A.; Raquez, J.-M.; Degée, P.; Dubois, P. Monomer−Linear Macromolecules−Cyclic Oligomers Equilibria in the Polymerization of 1,4-Dioxan-2-one. *Macromolecules* **2004**, *37* (1), 52−59.
(42) Bechtold, K.; Hillmyer, M. A.; Tolman, W. B. Perfectly Alternating Copolymer of Lactic Acid and Ethylene Oxide as a Plasticizing Agent for Polylactide. *Macromolecules* **2001**, *34* (25), 8641−8648.
(43) Mathisen, T.; Masus, K.; Albertsson, A. C. Polymerization of 1,5-dioxepan-2-one. II. Polymerization of 1,5-dioxepan-2-one and its cyclic dimer, including a new procedure for the synthesis of 1,5-dioxepan-2-one. *Macromolecules* **1989**, *22* (10), 3842−3846.
(44) McGuire, T. M.; Ning, D.; Williams, C. K. Using Differential Scanning Calorimetry to Accelerate Polymerization Catalysis: A Toolkit for Miniaturized and Automated Kinetics Measurements. *ACS Catal.* **2025**, *15* (9), 6760−6771.
(45) Kobayashi, S.; Nagayama, S.; Busujima, T. Lewis Acid Catalysts Stable in Water. Correlation between Catalytic Activity in Water and Hydrolysis Constants and Exchange Rate Constants for Substitution of Inner-Sphere Water Ligands. *J. Am. Chem. Soc.* **1998**, *120* (32), 8287−8288.
(46) Shannon, R. D. Revised effective ionic radii and systematic studies of interatomic distances in halides and chalcogenides. *Acta Crystallogr., Sect. A* **1976**, *32* (5), 751−767.
(47) Brown, P. L.; Ekberg, C. *Hydrolysis of Metal Ions*; Wiley, 2016.
(48) Eisenhardt, K. H. S.; Fiorentini, F.; Butler, F.; Thorogood, R.; Williams, C. K. General, Quantified Structure-Performance Correlations for Synergistic Heteronuclear Electro-, Polymerization, and Asymmetric Catalysts. *ACS Catal.* **2025**, *15* (15), 12959−12983.
(49) Kumar, A.; Lionetti, D.; Day, V. W.; Blakemore, J. D. Trivalent Lewis Acidic Cations Govern the Electronic Properties and Stability of Heterobimetallic Complexes of Nickel. *Chem.—Eur. J.* **2018**, *24* (1), 141−149.
(50) Reath, A. H.; Ziller, J. W.; Tsay, C.; Ryan, A. J.; Yang, J. Y. Redox Potential and Electronic Structure Effects of Proximal Nonredox Active Cations in Cobalt Schiff Base Complexes. *Inorg. Chem.* **2017**, *56* (6), 3713−3718.
(51) Butler, F.; Fiorentini, F.; Eisenhardt, K. H. S.; Williams, C. K. Structure-Activity Relationships for s-Block Metal/Co(III) Heterodinuclear Catalysts in Cyclohexene Oxide Ring-Opening Copolymerizations. *Angew. Chem., Int. Ed.* **2025**, *64* (12), No. e202422497.
(52) Fiorentini, F.; Diment, W. T.; Deacy, A. C.; Kerr, R. W. F.; Faulkner, S.; Williams, C. K. Understanding catalytic synergy in dinuclear polymerization catalysts for sustainable polymers. *Nat. Commun.* **2023**, *14* (1), 4783.

https://doi.org/10.1021/acscatal.5c08568
ACS Catal. 2026, 16, 5673−5681

(53) Brown, P. L.; Ekberg, C. Chapter 11 First Transition Series Metals. In *Hydrolysis of Metal Ions*; Brown, P. L., Ekberg, C., Eds.; Wiley, 2016; pp 499−716.
(54) Brown, P. L.; Ekberg, C. Chapter 8: Scandium, Yttrium and the Lanthanide Metals. In *Hydrolysis of Metal Ions*; Brown, P. L., Ekberg, C., Eds.; Wiley, 2016; pp 225−324.
(55) Nagae, H.; Aoki, R.; Akutagawa, S.-n.; Kleemann, J.; Tagawa, R.; Schindler, T.; Choi, G.; Spaniol, T. P.; Tsurugi, H.; Okuda, J.; et al. Lanthanide Complexes Supported by a Trizinc Crown Ether as Catalysts for Alternating Copolymerization of Epoxide and CO2: Telomerization Controlled by Carboxylate Anions. *Angew. Chem., Int. Ed.* **2018**, *57* (9), 2492−2496.
(56) Asaba, H.; Iwasaki, T.; Hatazawa, M.; Deng, J.; Nagae, H.; Mashima, K.; Nozaki, K. Alternating Copolymerization of CO2 and Cyclohexene Oxide Catalyzed by Cobalt−Lanthanide Mixed Multinuclear Complexes. *Inorg. Chem.* **2020**, *59* (12), 7928−7933.
(57) Handa, S.; Gnanadesikan, V.; Matsunaga, S.; Shibasaki, M. syn-Selective Catalytic Asymmetric Nitro-Mannich Reactions Using a Heterobimetallic Cu−Sm−Schiff Base Complex. *J. Am. Chem. Soc.* **2007**, *129* (16), 4900−4901.
(58) Handa, S.; Nagawa, K.; Sohtome, Y.; Matsunaga, S.; Shibasaki, M. A Heterobimetallic Pd/La/Schiff Base Complex for anti-Selective Catalytic Asymmetric Nitroaldol Reactions and Applications to Short Syntheses of β-Adrenoceptor Agonists. *Angew. Chem., Int. Ed.* **2008**, *47* (17), 3230−3233.
(59) Mihara, H.; Xu, Y.; Shepherd, N. E.; Matsunaga, S.; Shibasaki, M. A Heterobimetallic Ga/Yb-Schiff Base Complex for Catalytic Asymmetric α-Addition of Isocyanides to Aldehydes. *J. Am. Chem. Soc.* **2009**, *131* (24), 8384−8385.
(60) Xu, Y.; Lin, L.; Kanai, M.; Matsunaga, S.; Shibasaki, M. Catalytic Asymmetric Ring-Opening of meso-Aziridines with Malonates under Heterodinuclear Rare Earth Metal Schiff Base Catalysis. *J. Am. Chem. Soc.* **2011**, *133* (15), 5791−5793.
(61) Wood, Z. A.; Giri, M.; Min, H.; Ohanyan, A.; Guerrero, A.; Assefa, M. K.; Fieser, M. E. Effects of Lewis acidity and size of lanthanide salts for ring-opening copolymerization. *Chem. Commun.* **2025**, *61* (22), 4411−4414.
(62) Manjarrez, Y.; Clark, A. M.; Fieser, M. E. Rare Earth Metal-Containing Ionic Liquid Catalysts for Synthesis of Epoxide/Cyclic Anhydride Copolymers. *ChemCatChem* **2023**, *15* (12), No. e202300319.
(63) Hanrahan, K. V. M.; Meyers, C. M.; Vos, C. W.; Lin, J.-B.; Kozak, C. M. Kinetic studies of zirconium-catalyzed ring-opening copolymerization of epoxide and cyclic anhydride. *Can. J. Chem.* **2025**, *103*, 723.
(64) Jeong, Y.; Cho, M. K.; Seo, S.; Cho, H.; Son, K.-s.; Kim, H. Electronic Tuning of Iminotriphenolate Ligands for Titanium(IV)-catalyzed Ring-opening Copolymerization of Cyclic Anhydrides and Epoxides. *ChemCatChem* **2023**, *15* (3), No. e202201086.
(65) Raman, S. K.; Deacy, A. C.; Pena Carrodeguas, L.; Reis, N. V.; Kerr, R. W. F.; Phanopoulos, A.; Morton, S.; Davidson, M. G.; Williams, C. K. Ti(IV)-Tris(phenolate) Catalyst Systems for the Ring-Opening Copolymerization of Cyclohexene Oxide and Carbon Dioxide. *Organometallics* **2020**, *39* (9), 1619−1627.
(66) Cheng-Tan, M. D. C. L.; Wood, Z. A.; Fieser, M. E. Simplifying the problem: metal salts can be active and controlled catalysts in polyester synthesis. *Chem. Sci.* **2026**, *17* (2), 699−711.

https://doi.org/10.1021/acscatal.5c08568
ACS Catal. 2026, 16, 5673−5681